Monthly Notices
of the
ROYAL ASTRONOMICAL SOCIETY
MNRAS **443,** 1849–1860 (2014) doi:10.1093/mnras/stu1202

Multi-epoch high-spectral-resolution observations of neutral sodium in 14 Type Ia supernovae⋆

A. Sternberg,[1]†‡ A. Gal-Yam,[2] J. D. Simon,[3] F. Patat,[4] W. Hillebrandt,[1] M. M. Phillips,[5] R. J. Foley,[6] I. Thompson,[5] N. Morrell,[5] L. Chomiuk,[7] A. M. Soderberg,[8] D. Yong,[9] A. L. Kraus,[10] G. J. Herczeg,[11] E. Y. Hsiao,[5] S. Raskutti,[12] J. G. Cohen,[13] P. A. Mazzali[1,14] and K. Nomoto[15]

[1]*Max Planck Institute for Astrophysics, Karl Schwarzschild St. 1, D-85741 Garching bei München, Germany*
[2]*Benoziyo Center for Astrophysics, Faculty of Physics, Weizmann Institute of Science, Rehovot 76100, Israel*
[3]*Observatories of the Carnegie Institution for Science, 813 Santa Barbara St, Pasadena, CA 91101, USA*
[4]*European Southern Observatory, Karl Schwarzschild St. 2, D-85748 Garching bei München, Germany*
[5]*Carnegie Observatories, Las Campanas Observatory, Casilla 601 La Serena, Chile*
[6]*Department of Astronomy, University of Illinois Champagne-Urbana, MC-221, 1002 W. Green Street, Urbana, IL 61801, USA*
[7]*Department of Physics and Astronomy, Michigan State University, East Lansing, MI 48824, USA*
[8]*Harvard–Smithsonian Center for Astrophysics, 60 Garden Street, Cambridge, MA 02138, USA*
[9]*Research School of Astronomy and Astrophysics, Australian National University, Canberra, ACT 2611, Australia*
[10]*Department of Astronomy, The University of Texas at Austin, 2515 Speedway, Stop C1400, Austin, TX 78712-1205, USA*
[11]*Kavli Institute for Astronomy and Astrophysics, Peking University; Yi He Yuan Lu 5, Hai Dian Qu, Beijing 100871, China*
[12]*Department of Astrophysics, Princeton University, Princeton, NJ 08540, USA*
[13]*Department of Astrophysics, California Institute of Technology, MC 249-17, Pasadena, CA 91125, USA*
[14]*Astrophysics Research Institute, Liverpool John Moores University, Liverpool L3 5RF, UK*
[15]*Kavli Institute for the Physics and Mathematics of the Universe (WPI), The University of Tokyo, Kashiwa, Chiba 277-8583, Japan*

Accepted 2014 June 17. Received 2014 June 16; in original form 2013 November 14

ABSTRACT

One of the main questions concerning Type Ia supernovae is the nature of the binary companion of the exploding white dwarf. A major discriminant between different suggested models is the presence and physical properties of circumstellar material at the time of explosion. If present, this material will be ionized by the ultraviolet radiation of the explosion and later recombine. This ionization–recombination should manifest itself as time-variable absorption features that can be detected via multi-epoch high-spectral-resolution observations. Previous studies have shown that the strongest effect is seen in the neutral sodium D lines. We report on observations of neutral sodium absorption features observed in multi-epoch high-resolution spectra of 14 Type Ia supernova events. This is the first multi-epoch high-resolution study to include multiple SNe. No variability in line strength that can be associated with circumstellar material is detected in the events presented in this paper. If we include previously published events, we find that ∼18 per cent of the events in the extended sample exhibit time-variable sodium features associated with circumstellar material. We explore the implication of this study on our understanding of the progenitor systems of Type Ia supernovae via the current Type Ia supernova multi-epoch high-spectral-resolution sample.

Key words: circumstellar matter – supernovae: general – ISM: general.

1 INTRODUCTION

Type Ia supernovae (SNe Ia) are widely accepted to be the thermonuclear explosion of accreting carbon–oxygen white-dwarfs (WDs) in close binary systems (Hoyle & Fowler 1960). Despite numerous

⋆Partially based on observations made with ESO Telescopes at the La Silla Paranal Observatory, Chile, under programme. ID 289.D-5023, 290.D-5010, 290.D-5023, 091.D-0780.

† E-mail: asternberg@mpa-garching.mpg.de
‡ Minerva Fellow.

studies, the nature of the companion of the exploding WD still remains uncertain. Presently, there are two models that are widely accepted as plausible descriptions of SN Ia progenitor systems. In the first model, the single-degenerate (SD) model, the companion is a non-degenerate star that transfers mass on to the WD (Whelan & Iben 1973). In the second one, the double-degenerate (DD) model, the secondary is a WD, where the two WD spiral in due to gravitational-wave emission until they merge (Iben & Tutukov 1984; Webbink 1984). The double WD merger can either be a slow process that leads to a central ignition or, as some recent studies have showed, it may undergo a 'violent merger' with an off-centre ignition (Pakmor et al. 2012, 2013). A different DD channel is the WD collisions, in which two WD do not spiral in but rather collide head-on (Benz, Thielemann & Hills 1989; Raskin et al. 2009; Rosswog et al. 2009; Lorén-Aguilar, Isern & García-Berro 2010; Thompson 2011; García-Senz et al. 2013; Kushnir et al. 2013). A third model, less widely accepted at present, is the core-degenerate model in which a WD merges with the core of an evolved star during, or shortly after, the common-envelope phase (Sparks & Stecher 1974; Livio & Riess 2003; Kashi & Soker 2011; Ilkov & Soker 2012). One of the major differences between current alternative models is the properties of the gaseous environment surrounding the WD at the time of explosion. Therefore, detection of absorption by circumstellar material (CSM) in the spectra of SNe Ia, or the lack thereof, and the study of its properties might help to disentangle the plausible from the implausible progenitor systems.

Patat et al. (2007a, hereafter P07) were the first to report the detection of CSM in a SN Ia, SN 2006X, based on time-variability observed in the neutral sodium (Na I) D absorption lines (rest-frame wavelengths λλ5890, 5896). The lack of time variability in the Ca II H & K lines led P07 to conclude that the observed change in the sodium absorption features was due to the ionization and recombination of CSM, and not a geometrical line-of-sight effect. P07 based their conclusion arguing that SN Ia UV radiation is severely line-blocked by heavy elements bluewards of 3500 Å (Pauldrach et al. 1996; Mazzali 2000), and is therefore capable of ionizing only material that is relatively near the explosion. If the material density is sufficiently high, it will recombine after maximum light giving rise to variability in observed absorption features. They suggested an SD progenitor system for SN 2006X. Following P07, similar studies provided a mixture of results both of detection of time-variable absorption features associated with CSM – SN 2007le (Simon et al. 2009), SN 1999cl (Blondin et al. 2009, using low spectral resolution) and PTF 11kx (Dilday et al. 2012) – and of non-detection of such features – SN 2000cx (Patat et al. 2007b), SN 2007af (Simon et al. 2007). Patat et al. (2013) detected marginally significant time-variability in the sodium features of SN 2011fe that were anyway compatible with interstellar material (ISM) and not with CSM. This mixture of results suggests that SNe Ia might actually arise from two types of progenitor systems, as is suggested by other studies (Mannucci, Della Valle & Panagia 2006; Sullivan et al. 2010; Maguire et al. 2013; Wang et al. 2013). The published sample of SNe with multiple high-resolution spectra is too small to allow for a significant conclusion to be drawn. Moreover, it also prevents us from deriving a robust ratio between SNe Ia that show evidence of CSM and those that do not. For that, a larger sample of SN Ia multi-epoch high-resolution spectra is needed.

Sternberg et al. (2011, hereafter S11) adopted a different approach based on a statistical analysis of a single-epoch high-spectral-resolution sample consisting of 35 SN Ia events. S11 showed that SNe Ia in nearby spiral hosts exhibit a statistically significant over-abundance of features that are blueshifted relative to the strongest absorption feature, and this was interpreted as evidence of outflows from ∼20–25 per cent of their progenitor systems. Foley et al. (2012) showed that events classified as blueshifted à la S11 tend to have higher ejecta velocities and redder colours at maximum light compared to the rest of the SN Ia sample. Maguire et al. (2013) used a classification scheme slightly different than that used by S11 to analyse an extended sample consisting of the S11 sample and an additional 17 intermediate-resolution single-epoch spectra, showing a ∼20 per cent excess of events with blueshifted features. These analyses lend strong support to the existence of CSM in a non-negligible fraction of SNe Ia and the possibility of a bimodal distribution of SN Ia progenitors. Nevertheless, one cannot use the S11 sample or the Maguire et al. sample to study the properties of the CSM as it is not possible to confidently distinguish between CSM and ISM features for an individual SN in single-epoch spectra. Multi-epoch observations are needed.

In this paper, we present multi-epoch high-spectral-resolution observations of 14 Type Ia events, some of which are from the S11 sample for which only single-epoch spectra were previously published. Publication of such data will help make the published SN Ia multi-epoch high-spectral-resolution sample more complete. We use this data set, plus the previously published observations of six other SNe, to provide the first robust estimate of the fraction of SNe Ia exhibiting variable absorption. We discuss the robustness of the time-variability non-detection and how this effects the consistency of the current multi-epoch high-spectral-resolution sample with previous studies.

2 DATA

Observations were performed using either the Ultraviolet and Visual Echelle Spectrograph (UVES; Dekker et al. 2000) mounted on the Very Large Telescope array (VLT) UT2, the HIgh Resolution Echelle Spectrograph (HIRES; Vogt et al. 1994) mounted on the Keck I telescope, the Magellan Inamori Kyocera Echelle (MIKE; Bernstein et al. 2003) spectrograph mounted on the Magellan II Clay telescope, and the East Arm Echelle (EAE; Libbrecht & Peri 1995) spectrograph mounted on the 200 inch Hale telescope at Palomar. Information regarding the discovery and spectroscopic observations of individual SNe can be found in Appendix A. UVES data were reduced using the latest ESO Reflex reduction pipeline. HIRES spectra were reduced using the MAuna Kea Echelle Extraction (MAKEE) data reduction package (written by T. Barlow; http://spider.ipac.caltech.edu/staff/tab/makee/). MIKE spectra were reduced using the latest version of the MIKE pipeline (written by D. Kelson; http://code.obs.carnegiescience.edu/mike/). EAE data were reduced using standard IRAF routines.

3 RESULTS

Using the IRAF RVCORRECT and DOPCOR routines we applied the appropriate heliocentric correction to all the spectra. Using the IRAF SPLOT routine, we normalized the spectra, measured the rms and the signal-to-noise ratio (S/N) on the continuum in the vicinity of the D_2 and D_1 lines. We removed telluric features using a synthetic telluric spectrum produced by the Line By Line Radiative Transfer Model (Clough et al. 2005) based on the HITRAN data base (Rothman et al. 2009). For more details, see Patat et al. (2013, their appendix A). We measured the equivalent width (EW) of the absorption features using the rms as the *sigma0* parameter in the SPLOT error estimation. EW errors ignore continuum placement. Values of EW, error, S/N, and the D_1 to D_2 ratio for each epoch are

Table 1. Measurements for the observed events.

	Phase[a]	Instrument	EW (mÅ)		D_1/D_2[b]	S/N[c]
			D_2	D_1		
SN 2007on	+4	MIKE	4 ± 6	0 ± 5	N/A	116
	+61	HIRES	0 ± 8	0 ± 6	N/A	48
SN 2007sa	+66	HIRES	558 ± 11	475 ± 11	0.85	21
	+72	HIRES	538 ± 13	429 ± 13	0.8	18
SN 2007sr	+6	MIKE	152 ± 2	146 ± 2	0.96	109
	+7	MIKE	152 ± 2	137 ± 2	0.9	112
	+8	MIKE	152 ± 2	138 ± 2	0.91	117
	+10	EAE	152 ± 4	120 ± 4	0.79	51
	+30	HIRES	153 ± 2	126 ± 2	0.82	104
SN 2008C	+16	HIRES	637 ± 10	444 ± 10	0.7	34
	+22	HIRES	624 ± 15	423 ± 16	0.68	22
SN 2008dt	+6	HIRES	409 ± 33	287 ± 33	0.7	10
	+12	HIRES	490 ± 32	325 ± 32	0.66	11
	+18	HIRES	430 ± 25	354 ± 25	0.82	13
SN 2009ds	+7	MIKE	676 ± 5	497 ± 5	0.74	74
	+24	MIKE	704 ± 6	510 ± 6	0.72	68
SN 2010A	−8	MIKE	453 ± 3	308 ± 4	0.68	90
	−7	MIKE	456 ± 3	284 ± 4	0.62	88
	+14	MIKE	448 ± 7	301 ± 9	0.67	37
SN 2011iy	+64	MIKE	1314 ± 5	1066 ± 5	0.81	69
	+166	MIKE	1286 ± 26	1077 ± 25	0.84	13
SN 2012cu	+8	MIKE	928 ± 6	857 ± 6	0.92	79
	+24	MIKE	936 ± 7	851 ± 7	0.91	61
	+36	UVES	918 ± 6	838 ± 6	0.91	33
	+49	UVES	919 ± 8	851 ± 8	0.93	24
SN 2012fr	−5	UVES	0 ± 2	0 ± 2	N/A	111
	+7	UVES	0 ± 2	0 ± 2	N/A	119
	+18	UVES	0 ± 4	3 ± 4	N/A	83
	+39	UVES	9 ± 3	28 ± 3	N/A	102
	+96	MIKE	10 ± 11	18 ± 11	N/A	52
SN 2012hr	+7	MIKE	133 ± 3	102 ± 4	0.77	123
	+37	MIKE	122 ± 8	120 ± 9	0.98	45
SN 2012ht	−2	MIKE	0 ± 4	1 ± 4	N/A	148
	+5	UVES	3 ± 4	5 ± 4	N/A	67
	+7	MIKE	0 ± 9	0 ± 9	N/A	66
	+12	UVES	4 ± 7	5 ± 7	N/A	33
	+24	UVES	1 ± 3	0 ± 3	N/A	70
SN 2013aa	−1	MIKE	0 ± 3	0 ± 3	N/A	182
	+7	UVES	2 ± 3	0 ± 3	N/A	96
	+12	UVES	1 ± 2	0 ± 2	N/A	101
	+22	UVES	2 ± 3	1 ± 3	N/A	69
	+56	UVES	4 ± 5	2 ± 5	N/A	46
SN 2013aj	+3	UVES	89 ± 2	57 ± 2	0.64	73
	+35	UVES	83 ± 6	51 ± 6	0.62	28

[a]In days since *B*-band maximum light.
[b]For events that do not exhibit sodium lines the ratio is marked as N/A.
[c]Per pixel.

given in Table 1. Comparisons between the first epoch and every subsequent epoch obtained for each SN are presented in Figs 1–14. First epoch spectra are in blue and subsequent epochs in red. The black line in the narrow panel of each figure is the difference spectrum, i.e. the subtraction of the earlier epoch spectrum from the later one. For comparison, we present the EW, error and S/N measurements for SN 2006X, SN 2007le and PTF 11kx in Table 2.

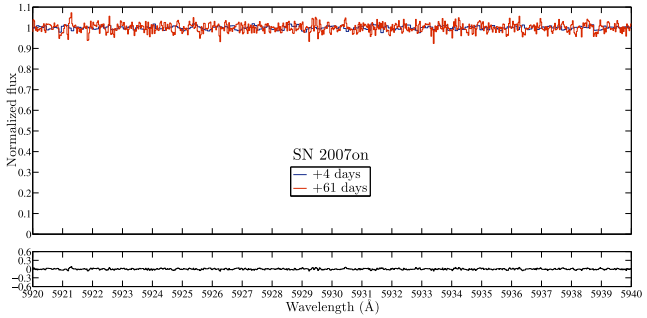

Figure 1. The dual-epoch spectra of SN 2007on. The first epoch is given in blue while the second is given in red. The difference spectrum (black line; in units of normalized flux) is given in the narrow panel at the bottom of the plot. Based on the host galaxy redshift, $z = 0.006\,494$, the host/SN Na I D features are expected to appear around 5928 and 5934 Å (for the D_2 and D_1, respectively). No features are observed.

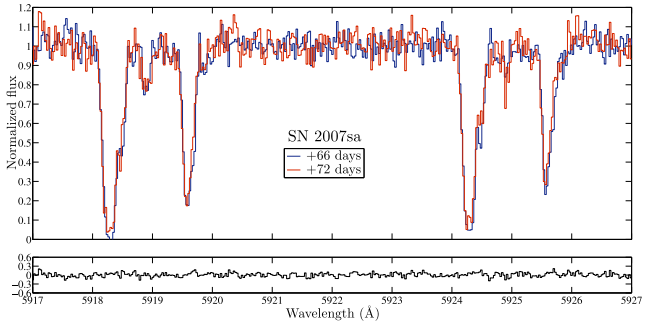

Figure 2. The dual-epoch spectra of SN 2007sa. The first epoch is given in blue while the second is given in red. The difference spectrum (black line) is given in the narrow panel at the bottom of the plot.

We performed the measurements for SN 2006X and PTF 11kx, and used the measurements previously published for SN 2007le (Simon et al. 2009). Fig. 15 shows a plot of the EW change as a function of days since maximum light for these three cases, SN 2007on, SN 2007C and SN 2011iy. The first spectrum of SN 2006X was obtained 2 d before maximum light. Therefore, we cannot determine whether or not changes occurred in the line profiles before maximum light. The spectra after day +61 do not exhibit variability. Moreover, the early variability in SN 2006X occurs in the strengthening of low-velocity features. Between day +14 and day +61 the line profiles undergo a radical change. The low-velocity features that intensified up to this point disappear, and higher velocity features appear. This behaviour is not observed in SN 2007le and PTF 11kx. The recombination time-scale for SN 2006X is of the order of 10 d. For SN 2007le, we see no visible variability between the spectra obtained at day −5 and at maximum light. The variability starts between maximum light and day +10, and stops sometime between day +12 and day +84. The first high-resolution spectrum of PTF 11kx is from day −1, and variability is observed between the first and second epoch. We cannot conclude whether or not pre-maximum variability occurred. Variability is not observed between day +20 and day +44, though S/N is very low. Therefore, the recombination time deduced from the PTF 11kx spectra is of the order of a few days. These three events have similar recombination time-scales, but exhibit different extent of variability. Moreover, while SN 2006X and SN 2007le exhibit variability only in their Na I D features, PTF 11kx exhibits variability in additional lines, including hydrogen.

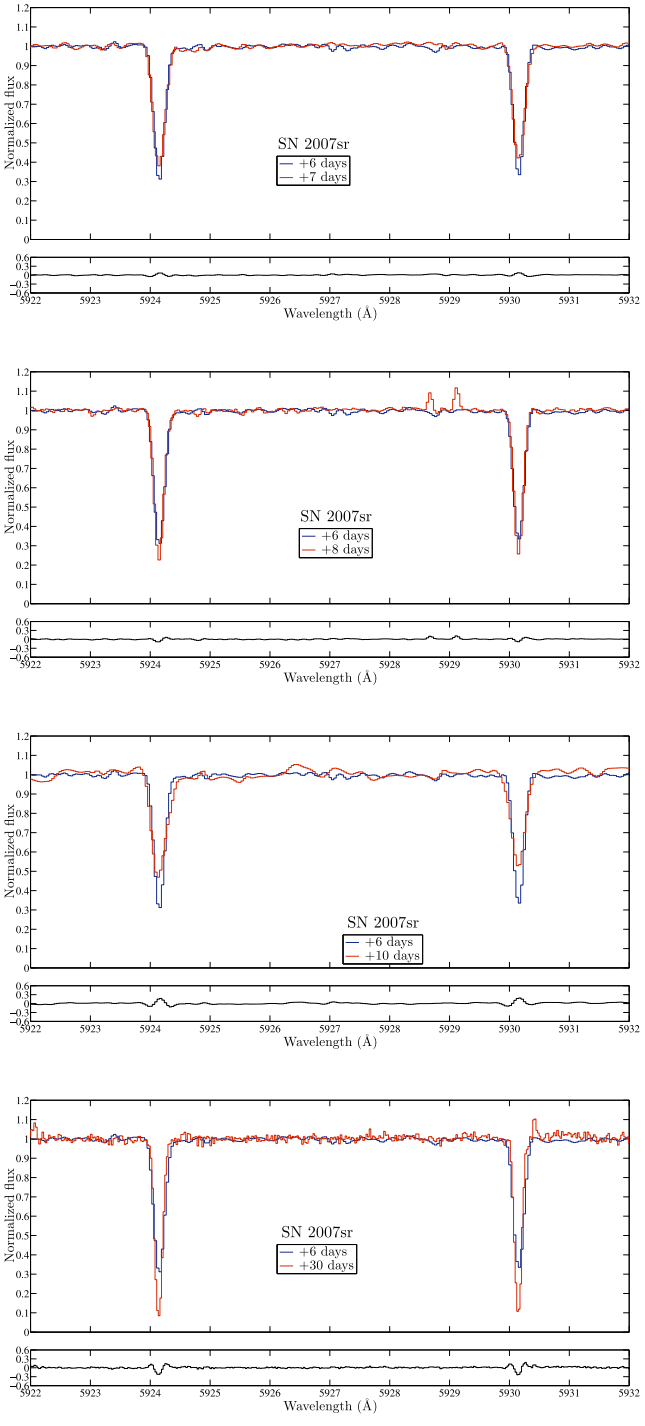

Figure 3. The multi-epoch spectra of SN 2007sr. Each plot shows a comparison of the first epoch (blue) and one of the other four epochs (red). The black lines given in the lower panel of each plot are the difference spectrum. As the measured EW of the different epochs are consistent with one another the observed difference in the line profiles are due to the different resolution of the spectrographs used on the different epochs.

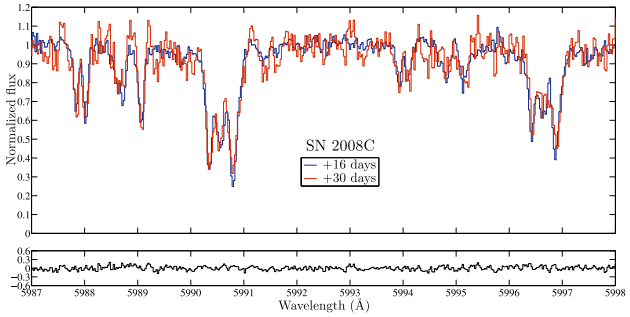

Figure 4. The dual-epoch spectra of SN 2008C. The first epoch is given in blue while the second is given in red. The difference spectrum (black line) is given in the narrow panel at the bottom of the plot.

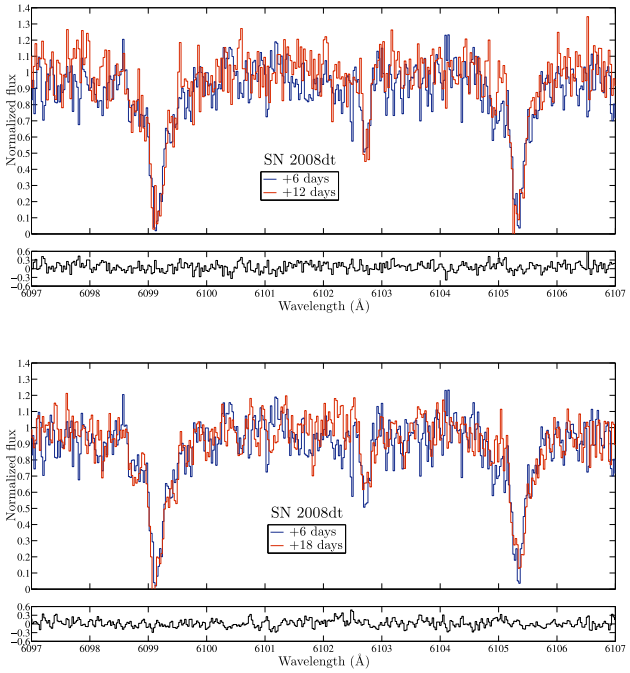

Figure 5. The triple-epoch spectra of SN 2008dt. Colour code is the same as in previous figures. The upper panel shows the first and second epochs and the middle panel shows the first and third.

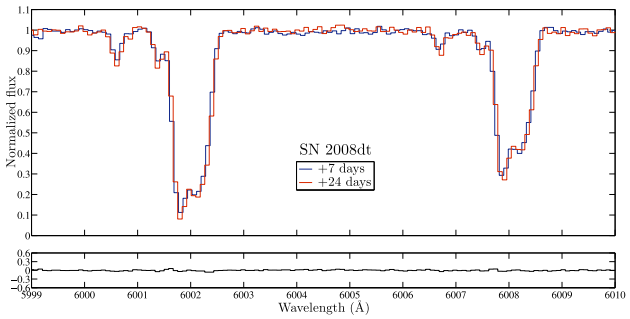

Figure 6. The dual-epoch spectra of SN 2009ds. Colour code is the same as in the previous figures.

In Fig. 1, we present a comparison between the two spectra of SN 2007on. Based on the host galaxy redshift, $z = 0.006\,494$ (Graham et al. 1998), the SN or host sodium features should have been visible, if present, within the given range. Both epochs seem to be featureless. The difference spectrum does not reveal any significant change between the two epochs. The EW values of the D_2 and D_1 lines are consistent with zero.

In Fig. 2, we present the region of the Na I D features observed in SN 2007sa spectra that are consistent with the SN or host galaxy redshift. Both epochs are overplotted to show that there is no

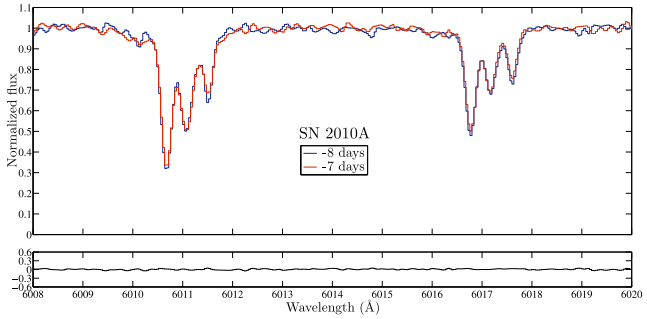

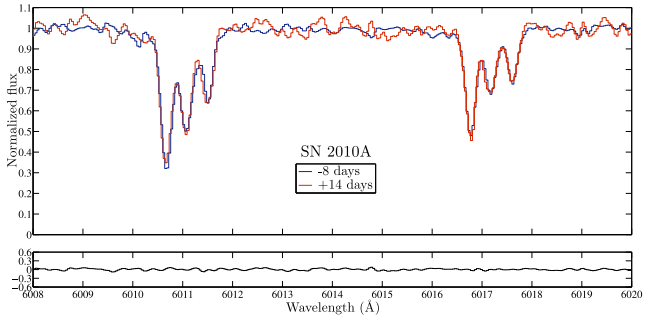

Figure 7. The triple-epoch spectra of SN 2010A.

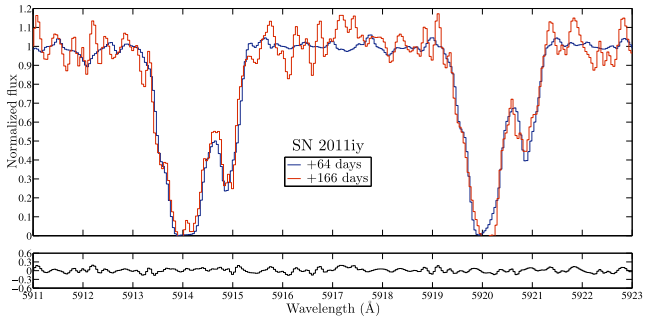

Figure 8. The dual-epoch spectra of SN 2011iy.

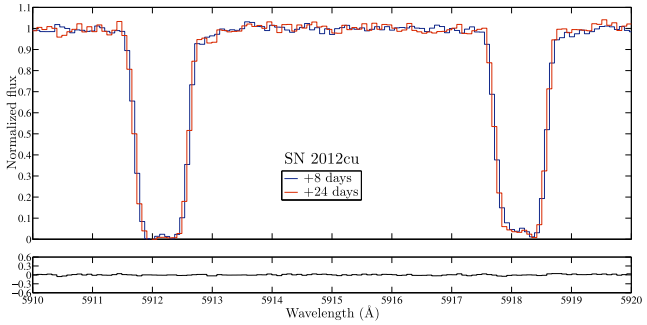

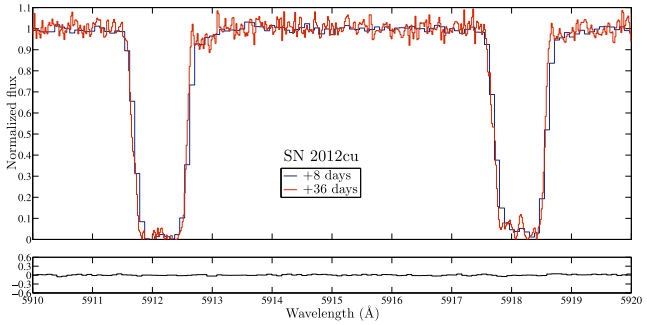

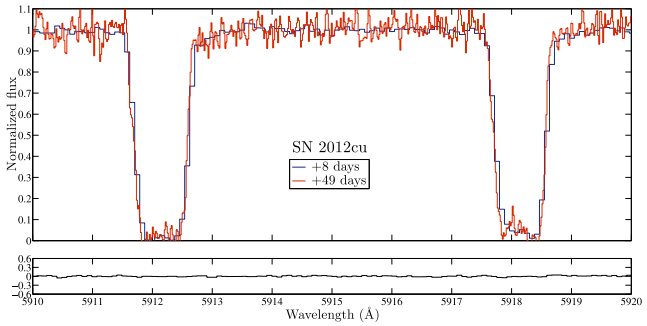

Figure 9. The multi-epoch spectra of SN 2012cu.

significant difference between them. Moreover, the difference spectrum does not reveal any significant change that is not within the noise level. Though the EW values of the D_2 and D_1 lines show a slight decreasing trend between the first and the second epoch they are still consistent within the calculated errors, 1.2 and 2.7σ for the D_2 and D_1 lines, respectively. Based on the time-scale of the variability observed in SN 2006X, SN 2007le and PTF 11kx an event with similar CSM environment is not expected to exhibit variability during the time period for which the two epochs of SN 2007sa have been obtained, let alone a decrease in line strength. Therefore, we consider it unlikely that these changes are real.

In Fig. 3, we present the sodium region of the multi-epoch spectra of SN 2007sr. These five epochs were obtained using three different spectrographs – MIKE, EAE, and HIRES. Though some apparent variability can be seen, the D_2 EW values measured for all epochs are all consistent within the calculated errors. The changes in the D_1 measurements in the fourth and fifth epochs are close to the 4σ level but are most likely not real, rather due to normalization of the spectrum near the edge of the D_1 line, and they do not appear in the stronger D_2 lines. The observed variability can be attributed to the difference between the spectral resolution of the three instruments.

An examination of the SN 2008C spectra in Fig. 4 does not reveal features that are significantly variable in both lines of the sodium doublet. Though the EW values exhibit a slight decreasing trend they are consistent with one another as they are in agreement within $\sim$1σ. In addition, the decrease in EW is contrary to the expected behaviour from ionization–recombination. Rather, this decrease, if it were significant, would be consistent with ongoing ionization at epochs that are a 16 and 22 d after maximum light.

Each panel of Fig. 5 shows comparisons between second (upper) or third (lower) epoch and the first epoch of SN 2008dt. Though some lines exhibit a visible change, these changes are all within the variations expected due to noise. This can be seen quite clearly in the difference spectra. Moreover, when we examine the EW values, we see that the D_2 and the D_1 line seem to show different trends. As the sodium D lines are a doublet, a real trend should manifest itself in the same manner in both lines. Moreover, given the error estimates the EW values of the three epochs are consistent with one another well within the 2σ level.

The dual-epochs of SN 2009ds are presented in Fig. 6. The difference spectra given in the lower panel demonstrate that the slight changes between the two epochs are well within the noise level. EW values of the D_1 lines are consistent with one another. The EW values of the D_2 show a larger difference and an agreement of only

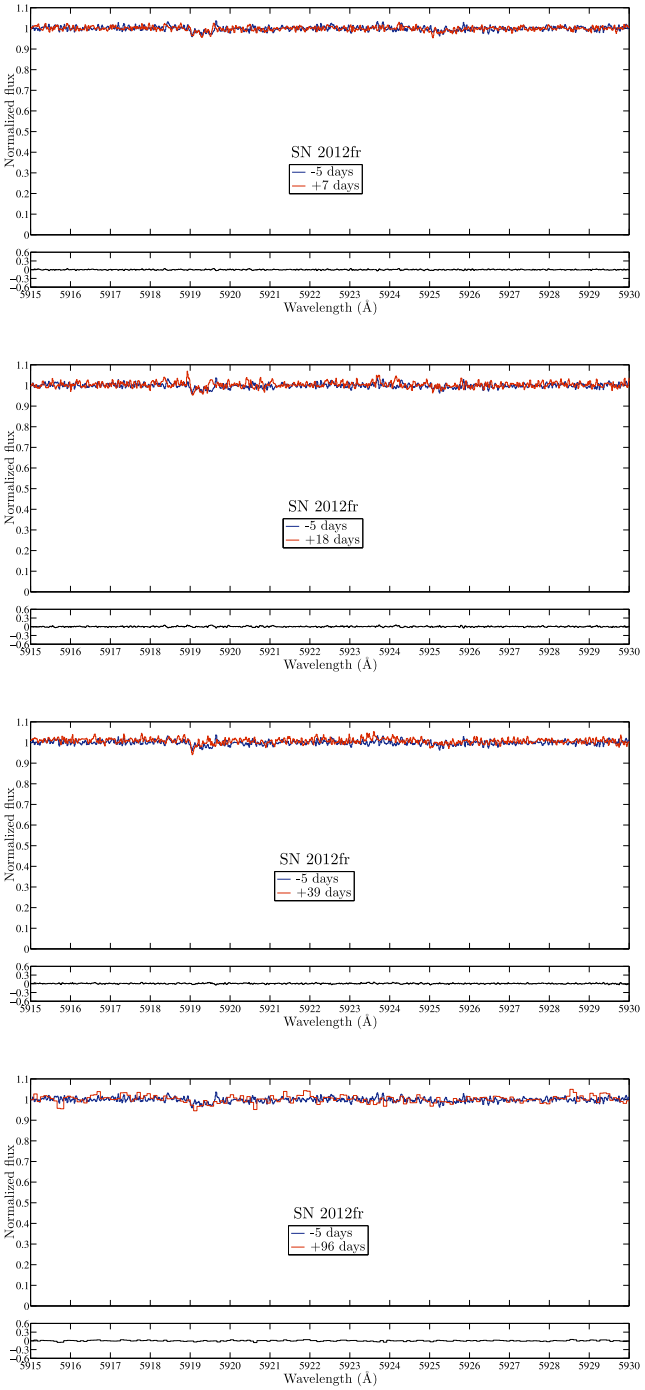

Figure 10. The multi-epoch spectra of SN 2012fr. SN or galaxy ($z = 0.005\,457$) Na I D features are expected to appear around 5922 and 5928 Å (D_2 and D_1, respectively). The very weak features around 5919 Å are slightly undersubtracted telluric features. No host or SN features are observed.

3.6σ. If we look at the EW of the D_1 and D_2 lines combined, we see that the two epoch show a difference of 3.7σ. This is a small but significant detection of time variability. Whether or not this variability can be associated with CSM will be discussed in Section 4. The two epochs are spread over a period that spans the time-variability period detected for SN 2006X, SN 2007le and PTF 11kx.

Examination of Fig. 7 does not reveal significant variations in the absorption line profiles observed in the spectra of SN 2010A. All variations in the D_2 lines are in agreement with the S/N and the calculated errors, at the 1σ level or below. However, the EW of the D_1 lines of the second epoch does not agree with the first epoch at a 4σ level. Nevertheless, the EW of the D_1 lines in the second and third epoch agree on a 1.7σ level and between the first and third epoch on a 0.7σ level. Moreover, if this variability were true, the stronger D_2 lines should have shown a greater disagreement, yet they do not.

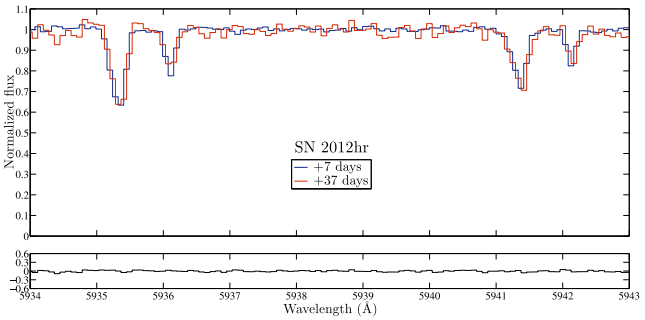

Figure 11. The dual-epoch spectra of SN 2012hr. The observed variability in the D_2 red-most feature (~5936.05 Å) is both not observed in the corresponding D_1 line and within the calculated errors.

The second epoch of SN 2011iy was obtained with very poor S/N. Even though some variability is seen in Fig. 8, the difference spectrum shows that the difference is well within the noise level. The variations in the absorption lines are of the same order as the variations seen in the continuum between the doublets. Moreover, the values of the EW are in agreement within 1.1σ.

All four epochs of SN 2012cu seem to be well in agreement with one another as seen in Fig. 9. The EW values also agree with each other quite well. The largest disagreement is a 2.3σ difference between the EW of the D_1 features measured for the first and third epochs. The lines are highly saturated. Under such conditions, the optically-thick regime, the EW is proportional to the square root of the number of absorbers along the line-of-sight. Large variation in Na I is needed for a small change in EW.

There are some very weak features around 5919 Å in the spectra of SN 2012fr (see Fig. 10). These are slightly undersubtracted telluric features. Otherwise the region seems to be featureless on all epochs. Childress et al. (2013) report a 3σ upper limit of 42 mÅ for the Na I D_2 line, and 40.8 mÅ, and use it to give a low upper limit to the reddening. The limits reported here are even more stringent. SN 2012ht and SN 2013aa also exhibit featureless spectra, see Figs 12 and 13, respectively.

The spectra of SN 2012hr are presented in Fig. 11. We can see that the comparison between the two epochs does not reveal significant variability. Though the red-most D_2 feature shows a slight decrease in intensity this is not observed in the D_1 feature. In addition, the EW values of the D_2 features are consistent within a 1.3σ level.

The two epochs of SN 2013aj are presented in Fig. 14. While the blue-most feature of the sodium doublet appears to experience some strengthening, the EWs of both epochs agree with each other within the 1σ level. Moreover, the difference spectrum shows that the differences are within the noise level.

In addition to the NA ID lines, we also examined the Ca II H&K and K I lines for variability. In about half of the cases, the S/N is too low to determine whether or not the calcium features vary or not. In the rest of the cases, we do not observed time-variability of more than 3σ in any of the features (simultaneously in both the H and the K lines). The UVES spectra do not cover the K I region. We do not observe variability in the HIRES and/or MIKE spectra

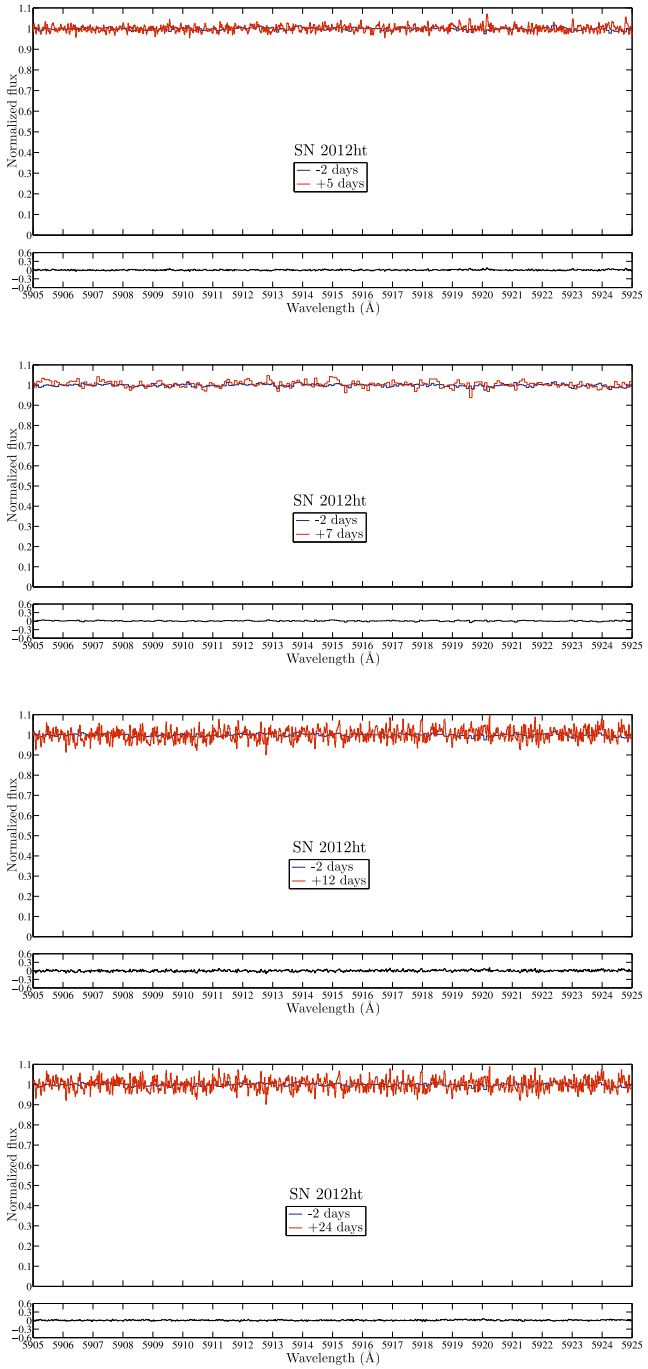

Figure 12. The multi-epoch spectra of SN 2012ht. SN or host galaxy ($z = 0.003\,559$) Na I D features are expected to appear around 5911 and 5917 Å. No features are observed.

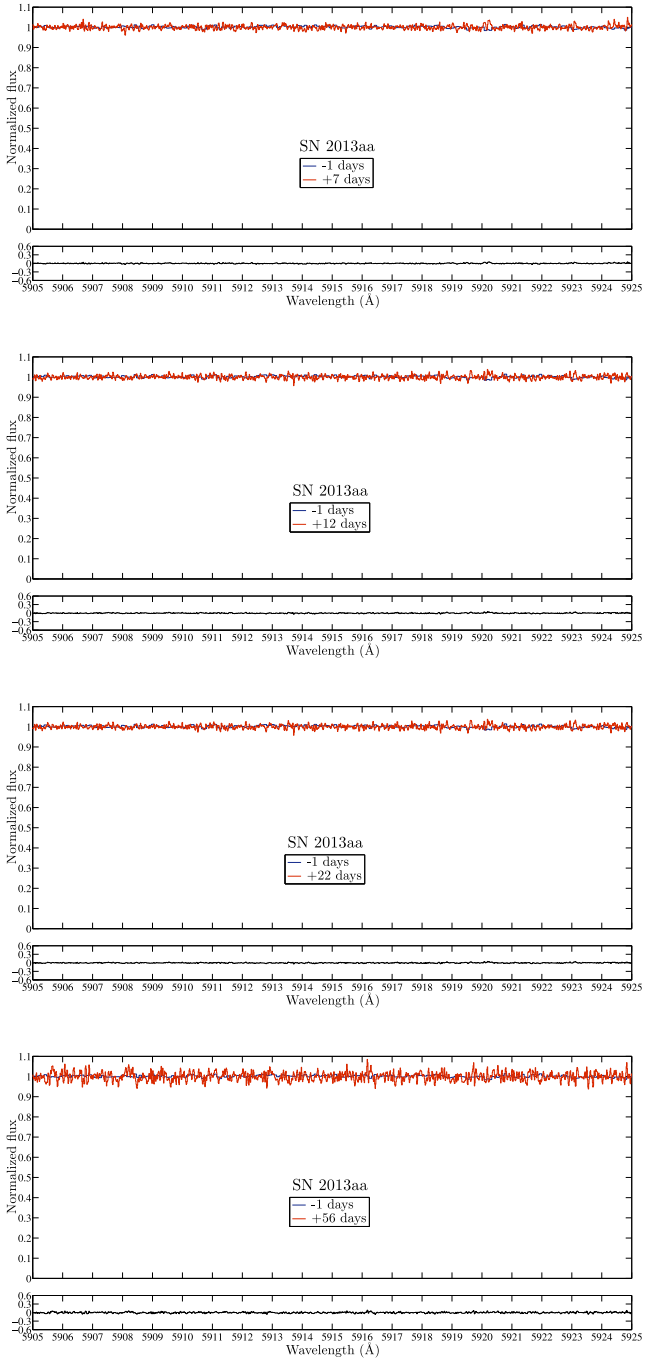

Figure 13. The multi-epoch spectra of SN 2013aa. SN or host galaxy ($z = 0.003\,999$) Na I D features are expected to appear around 5913.5 and 5919.5 Å. No features are observed.

seven events, and for two events the S/N was too low. Therefore, for events with sufficient quality of data, we can report that these lines do not exhibit significant time-variability.

To summarize, 13 of the SNe Ia presented in this study do not exhibit significant time-variable absorption features that could be indicative of the presence of CSM along the line of sight to these events. The difference spectra of these events are consistent with zero within the S/N. In contrast, an examination of SN 2006X, SN 2007le and PTF 11kx, the three previously published events for which time-variability was detected in high-resolution spectra, clearly reveals the time-variability in the Na I D absorption features. One SN, 2009ds, does indeed exhibit variability. This variability is not as profound as the variability exhibited in the previously published detections, and in the next section we will discuss whether this variability is indicative of CSM or whether it is consistent with other explanations.

4 DISCUSSION

Comparing the shape and EW of the sodium D line features exhibited in the SN Ia events presented in this study reveals no

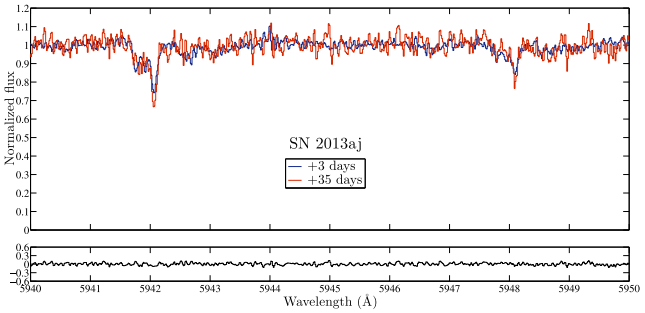

Figure 14. The dual-epoch spectra of SN 2013aj.

Table 2. Measurements for the previously published events.

	Phase[a]	EW (mÅ)		S/N[b]
		D_2	D_1	
SN 2006X[c]	−2	828 ± 3	688 ± 3	78
	14	1137 ± 2	882 ± 2	101
	61	1206 ± 4	947 ± 4	56
	121	1147 ± 12	918 ± 12	20
SN 2007le[d]	−5	894 ± 3	649 ± 3	113
	0	883 ± 4	661 ± 5	71
	10	906 ± 20	695 ± 20	16
	12	949 ± 4	702 ± 5	76
	84	1006 ± 7	766 ± 7	46
PTF 11kx[c, e]	−1	75 ± 13	124 ± 13	21
	9	172 ± 12	91 ± 12	24
	20	292 ± 20	190 ± 20	14
	44	199 ± 19	183 ± 19	15

[a]In days since *B*-band maximum light.
[b]Per pixel.
[c]New measurements.
[d]Taken from Simon et al. (2009).
[e]Measured only on the variable features.

significant time-variability that may be associated with CSM in all but one case, SN 2009ds. A question immediately arises what is the cause of this variability. The measured change in EW is $\Delta EW_{D_2} = 28 \pm 8$ mÅ and $\Delta EW_{D_1} = 13 \pm 8$ mÅ. This change is small compared to the variability observed in SN 2006X (∼350 Å and 250 mÅ, respectively[1]), SN 2007le and PTF 11kx (for both cases ΔEW ∼ 100 mÅ in each of the doublet lines). It is comparable to the observed variability in SN 2011fe, $\Delta EW_{D_2} = 15.6 \pm 6.5$ mÅ (Patat et al. 2013), which was shown to be consistent with the expected short time-scale variations in interstellar absorptions produced by an expending SN photosphere combined with a patchy ISM (Patat et al. 2010). Therefore, even if the observed variability is real, we conclude that it is most likely associated with the ISM and not to the CSM environment of SN 2009ds.

A question that needs addressing is whether the reported non-detections are robust or not. A robust non-detection should have an early first epoch that can serve as a good zero-point with which to compare later epochs. As the CSM, if present, begins to recombine after maximum light, the initial epoch should be obtained around maximum light. An initial spectrum obtained later, might have been obtained after some, or all, of the CSM has recombined, and will not serve as a good zero-point for comparison.

[1] Using the average of the third and fourth epochs.

The first spectra of both SN 2007sa and SN 2011iy were obtained more than 60 d after maximum light. Based on previous CSM detections, we expect that by this phase any CSM that was ionized by the UV flash will have already re-combined (see Fig. 15). Therefore, such late spectra cannot rule out variability at earlier stages and therefore should not be used as a non-detection and should not be included in statistical analysis of multi-epoch high-spectral-resolution samples of SNe Ia.

Based on previous cases (SN 2006X, SN 2007le and PTF 11kx), we cannot determine that any variability would have been seen between the two closely-spaced epochs we have for SN 2008C (days +18 and +22; see Fig. 15). So, we argue that this non-detection should not be considered robust. This case emphasizes the need for an early-time first epoch and at least on more well-spaced epoch.

The first epochs of the remaining 11 events were obtained no later than 8 d after maximum light. If we disregard epochs of SN 2006X, SN 2007le and PTF 11kx that were obtained earlier than 8 d, we can still observe significant time-variability in all three events. Therefore, we argue that the non-detection reported for these events are robust. This criterion will have to be revised if future observations will show events for which all the time-variability occurs earlier than 8 d after maximum light.

The D_1/D_2 ratio for many of our events is considerably larger than 0.5, the ratio for optically thin gas. In the optically thick regime the line profiles are less sensitive to changes in the column density, making them harder to identify, especially in low S/N spectra. Nevertheless, the obvious fact that we do not observe time variability in the spectra of these events at these epochs is an indication that the environment along the line of sight to these events is different with respect to that along the line of sight to SN 2006X, SN 2007le and PTF 11kx.

In addition, we cannot rule out the presence of weak absorption lines that will be undetectable due to the noise in the spectra. Following Leonard & Filippenko (2001), one can quantify the upper detection limit when no features are apparent in the spectrum as,

$$W_\lambda(3\sigma) = 3\Delta\lambda\Delta I\sqrt{\frac{W_{\rm line}}{\Delta\lambda}}\sqrt{\frac{1}{B}}, \quad (1)$$

where $\Delta\lambda$ is the spectral resolution, ΔI the root-mean-square fluctuations of the normalized flux, $W_{\rm line}$ is the width of the feature, and B is the number of bins per resolution element. Assuming that these lines are optically thin, we can follow (Spitzer 1978, section 3.4.c) and use the curve-of-growth to convert EW into column densities using,

$$N = \frac{m_e c^2}{\pi e^2}\frac{W_\lambda}{f\lambda^2} = 1.13\times10^{20}\frac{W_\lambda}{f\lambda^2}, \quad (2)$$

where f is the oscillator strength. Given the different spectral resolution of the different instruments and the S/N of the different observations, and assuming $W_\lambda = 0.2$ Å, we can conclude that any feature arising from a Na I column density of more than a few times 10^{10} cm^{-2} should have been detectable in the spectra of the majority of these events. The extreme cases are SN 2012fr, for which the detectability limit is $\sim 7.8\times10^9$ cm^{-2} and SN 2007on and SN 2008dt, for which the limits are 6×10^{10} and 8×10^{10} cm^{-2}, respectively. Therefore, a line-of-sight environment similar to those observed for SN 2006X, SN2007le and PTF 11kx should have produced detectable lines. Assuming all the sodium is neutral and a solar abundance ratio, $\log {\rm Na/H} = -6.3$, we get a hydrogen column

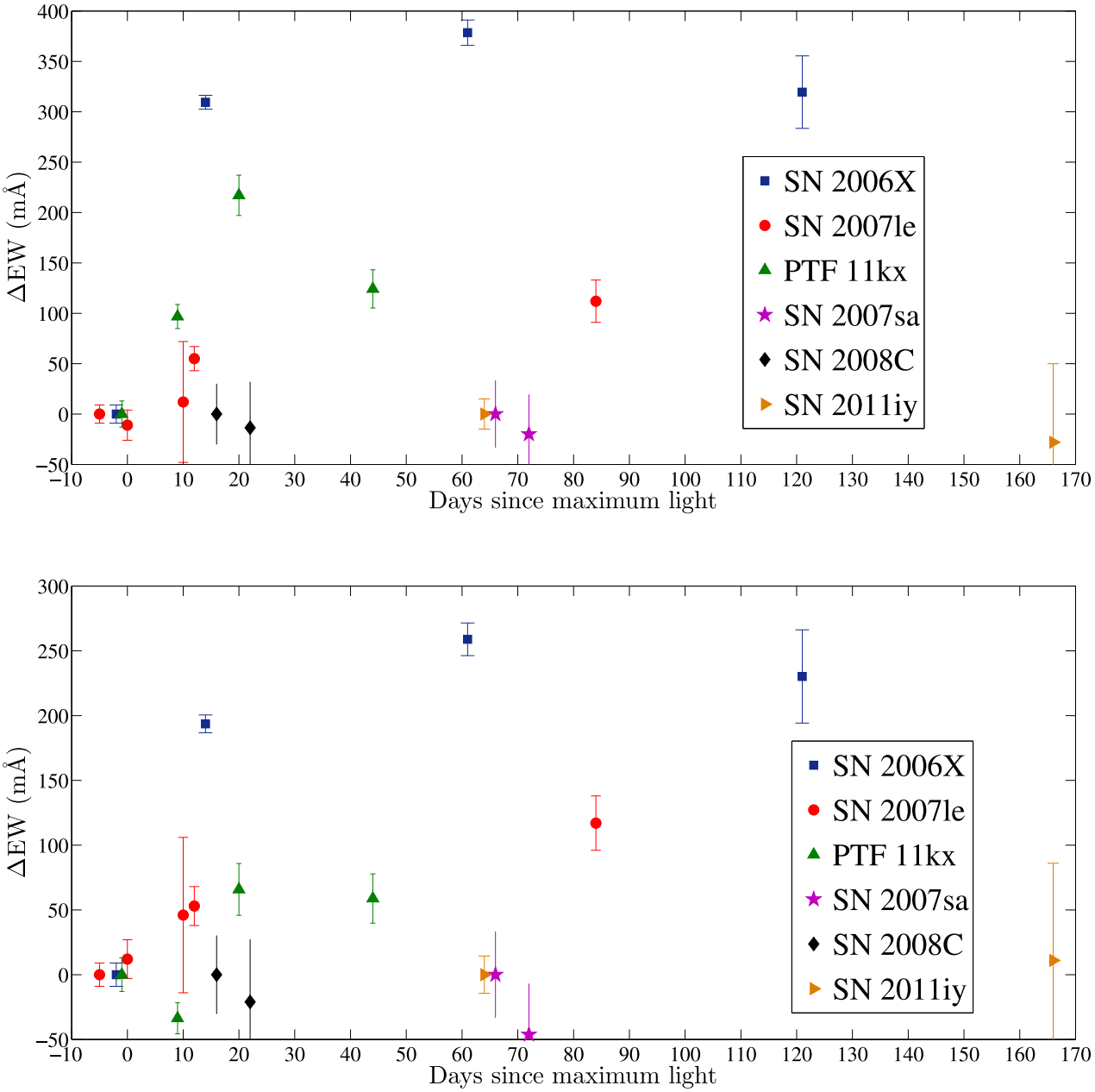

Figure 15. Changes in the EW of previously published events SN 2006X, SN 2007le and PTF 11kx as a function of days since maximum light. The upper panel presents the change in the D_2 line and the lower in the D_1 lines. The error bars represent 3σ errors. The data points for SN 2007sa, SN 2008C and SN 2011iy are plotted to show that their observations were either performed on epochs too closely spaced apart or that their first epochs were obtained too late.

density limit of $\sim 10^{17}$ cm^{-2}. Assuming this material is distributed in a thin spherical shell at radius R the mass of the shell will be,

$$M_{\rm shell} \simeq \left(\frac{R}{10^{17}\,{\rm cm}}\right)^2 \times 10^{-5}\,{\rm M}_{\odot}, \quad (3)$$

though this estimate is only a rough estimate and most likely an over estimate. For SN 2012fr the limit is approximately one order of magnitude lower.

Our spectroscopic observations only probe the CSM along the line of sight, therefore, we cannot rule out presence of material off the line of sight. Nevertheless, simulations of proposed progenitor systems (e.g. Mohamed, Booth & Podsiadlowski 2013; Raskin & Kasen 2013; Shen, Guillochon & Foley 2013) may offer an insight to whether they can form CSM in a way that allows for line-of-sight environments that are consistent with our observations, especially the relatively clean featureless line of sights observed towards SN 2007on, SN 2012fr, SN 2012ht and SN 2013aa. Such a comparison between theoretical results and the observed multi-epoch high-spectral-resolution sample can be highly insightful, but remains beyond the scope of this paper.

5 CONCLUSIONS

Our data extends the published multi-epoch high-spectral-resolution sample size to 17 events for which robust detection or non-detection can be claimed. Three events exhibit time-variable Na I D features attributed to CSM. Assuming Poisson statistics, we find that 18 ± 11 per cent of the events in the enlarged sample exhibit time-variable

features that can be associated with CSM. S11 and Maguire et al. (2013) estimated the fraction of SNe Ia with CSM to be 20–25 per cent of nearby SNe Ia in late-type galaxy hosts. For consistency sake, we exclude SN 2007on which occurred in an elliptical host and get 19 ± 12 per cent, which is consistent with the previous results. This estimate is a lower limit, as CSM may lay off the line of sight or on the line of sight but further away from the progenitor system. In the first case, this material will not be visible in the spectrum. In the later, the CSM lines will not vary with time and be regarded as a non-detection. Moreover, though this is the largest multi-epoch high-spectral-resolution SN Ia sample to date, it is still relatively small. A larger sample will be useful to shed light on the ratio between SNe Ia with CSM and those without. This ratio and the study of the properties of detected CSM can help us to disentangle the different proposed channels leading to SNe Ia explosions. In order for the published multi-epoch high-spectral-resolution sample to be more complete and not biased towards events with detected time-variability it is critical to publish all the observed events. With the publication of this data set, the sample of SNe Ia observed by our team's Keck-Magellan effort till 2009 is complete. The VLT 2008–2009 sample is still being worked on and will be soon published (Cox et al., in preparation).

ACKNOWLEDGEMENTS

We thank the anonymous referee for his comments that help us improve our paper.

AS is supported by a Minerva Fellowship. The research of AG is supported by the EU/FP7 via an ERC grant no. 307260, the Minerva ARCHES prize and the Kimmel award.

The authors would like to acknowledge the generosity of the late Wallace L. W. Sargent in providing data. The authors would also like to acknowledge the help of D. J. Osip and J. F. Steiner in obtaining the data.

Partially based on observations made with ESO Telescopes at the La Silla Paranal Observatory, Chile, under programme ID 289.D-5023, 290.D-5010, 290.D-5023, 091.D-0780.

This paper includes data gathered with the 6.5 metre Magellan Telescopes located at Las Campanas Observatory, Chile.

Some of the data presented herein were obtained at the W.M. Keck Observatory, which is operated as a scientific partnership among the California Institute of Technology, the University of California and the National Aeronautics and Space Administration. The Observatory was made possible by the generous financial support of the W.M. Keck Foundation. The authors wish to recognize and acknowledge the very significant cultural role and reverence that the summit of Mauna Kea has always had within the indigenous Hawaiian community. We are most fortunate to have the opportunity to conduct observations from this mountain.

REFERENCES

Agnoletto I., Harutyunyan A., Benetti S., Turatto M., Cappellaro E., Dennefeld M., Adami C., 2007, Cent. Bur. Electron. Telegrams, 1163, 1

Anderson J., Morrell N., Folatelli G., Stritzinger M., 2009, Cent. Bur. Electron. Telegrams, 1789, 1

Ayani K., Yamaoka H., 2008, Cent. Bur. Electron. Telegrams, 1197, 1

Benz W., Thielemann F.-K., Hills J. G., 1989, ApJ, 342, 986

Bernstein R., Shectman S. A., Gunnels S. M., Mochnacki S., Athey A. E., 2003, in Iye M., Moorwood A. F. M., eds, Proc. SPIE Conf. Ser. Vol. 4841, Instrument Design and Performance for Optical/Infrared Ground-based Telescopes. SPIE, Bellingham, p. 1694

Blondin S., Berlind P., 2008, Cent. Bur. Electron. Telegrams, 1424, 1

Blondin S., Prieto J. L., Patat F., Challis P., Hicken M., Kirshner R. P., Matheson T., Modjaz M., 2009, ApJ, 693, 207

Brimacombe J. et al., 2013, Cent. Bur. Electron. Telegrams, 3434, 1

Challis P., Calkins M., 2009, Cent. Bur. Electron. Telegrams, 1788, 2

Childress M., Zhou G., Tucker B., Bayliss D., Scalzo R., Yuan F., Schmidt B., 2012, Cent. Bur. Electron. Telegrams, 3275, 2

Childress M. J. et al., 2013, ApJ, 770, 29

Clough S. A., Shephard M. W., Mlawer E. J., Delamere J. S., Iacono M. J., Cady-Pereira K., Boukabara S., Brown P. D., 2005, J. Quant. Spectrosc. Radiat. Transfer, 91, 233

Cox L., Newton J., Puckett T., Orff T., 2010, Cent. Bur. Electron. Telegrams, 2109, 1

Dekker H., D'Odorico S., Kaufer A., Delabre B., Kotzlowski H., 2000, in Iye M., Moorwood A. F., eds, Proc. SPIE Conf. Ser. Vol. 4008, Optical and IR Telescope Instrumentation and Detectors. SPIE, Bellingham, p. 534

Dilday B. et al., 2012, Science, 337, 942

Drake A. J., Djorgovski S. G., Williams R., Mahabal A., Graham M. J., Christensen E., Beshore E. C., Larson S. M., 2007, Astron. Telegram, 1337, 1

Drescher C. et al., 2012, Cent. Bur. Electron. Telegrams, 3346, 1

Foley R. J., Esquerdo G., 2010, Cent. Bur. Electron. Telegrams, 2112, 1

Foley R. J. et al., 2012, ApJ, 752, 101

Gal-Yam A., Simon J., Klotz A., Rosolowsky E., 2007, Astron. Telegram, 1263, 1

García-Senz D., Cabezón R. M., Arcones A., Relaño A., Thielemann F. K., 2013, MNRAS, 436, 3413

Graham A. W., Colless M. M., Busarello G., Zaggia S., Longo G., 1998, A&AS, 133, 325

Hoyle F., Fowler W. A., 1960, ApJ, 132, 565

Iben I., Jr, Tutukov A. V., 1984, ApJS, 54, 335

Ilkov M., Soker N., 2012, MNRAS, 419, 1695

Itagaki K., Brimacombe J., Noguchi T., Nakano S., 2011, Cent. Bur. Electron. Telegrams, 2943, 1

Itagaki K. et al., 2012, Cent. Bur. Electron. Telegrams, 3146, 1

Kashi A., Soker N., 2011, MNRAS, 417, 1466

Klotz A. et al., 2012, Cent. Bur. Electron. Telegrams, 3275, 1

Kushnir D., Katz B., Dong S., Livne E., Fernández R., 2013, ApJ, 778, L37

Leonard D. C., Filippenko A. V., 2001, PASP, 113, 920

Libbrecht K. G., Peri M. L., 1995, PASP, 107, 62

Livio M., Riess A. G., 2003, ApJ, 594, L93

Lorén-Aguilar P., Isern J., García-Berro E., 2010, MNRAS, 406, 2749

Madison D., Li W., Filippenko A. V., 2008, Cent. Bur. Electron. Telegrams, 1423, 1

Maguire K. et al., 2013, MNRAS, 436, 222

Mannucci F., Della Valle M., Panagia N., 2006, MNRAS, 370, 773

Marion G. H., Milisavljevic D., Rines K., Wilhelmy S., 2012, Cent. Bur. Electron. Telegrams, 3146, 2

Mazzali P. A., 2000, A&A, 363, 705

Mohamed S., Booth R., Podsiadlowski P., 2013, in Krzesiński J., Stachowski G., Moskalik P., Bajan K., eds, ASP Conf. Ser. Vol. 469, Proc. 18th European White Dwarf Workshop. Astron. Soc. Pac., San Francisco, p. 323

Morrell N., Phillips M. M., Contreras C., Roth M., Hsiao E. Y., Marion G. H., Stritzinger M., 2012, Astron. Telegram, 4663, 1

Mostardi R., Li W., 2007, Cent. Bur. Electron. Telegrams, 1161, 1

Naito H., Sakane Y., Anan T., Kouzuma S., Yamaoka H., 2007, Cent. Bur. Electron. Telegrams, 1173, 1

Nakano S., Itagaki K., Kadota K., Wells W., Nissinen M., Hentunen V.-P., 2009, Cent. Bur. Electron. Telegrams, 1784, 1

Pakmor R., Kromer M., Taubenberger S., Sim S. A., Röpke F. K., Hillebrandt W., 2012, ApJ, 747, L10

Pakmor R., Kromer M., Taubenberger S., Springel V., 2013, ApJ, 770, L8

Parker S., Amorim A., Parrent J. T., Sand D., Valenti S., Graham M. L., Howell D. A., 2013, Cent. Bur. Electron. Telegrams, 3416, 1

Parrent J. T., Sand D., Valenti S., Graham M. J., Howell D. A., 2013, Astron. Telegram, 4817, 1

Patat F. et al., 2007a, Science, 317, 924 (P07)
Patat F. et al., 2007b, A&A, 474, 931
Patat F., Cox N. L. J., Parrent J., Branch D., 2010, A&A, 514, A78
Patat F. et al., 2013, A&A, 549, A62
Pauldrach A. W. A., Duschinger M., Mazzali P. A., Puls J., Lennon M., Miller D. L., 1996, A&A, 312, 525
Pojmanski G., Prieto J. L., Stanek K. Z., Beacom J. F., 2008, Cent. Bur. Electron. Telegrams, 1213, 1
Pollas C., Klotz A., 2007, Cent. Bur. Electron. Telegrams, 1121, 1
Puckett T., Gagliano R., Newton J., Orff T., 2008, Cent. Bur. Electron. Telegrams, 1195, 1
Raskin C., Kasen D., 2013, ApJ, 772, 1
Raskin C., Timmes F. X., Scannapieco E., Diehl S., Fryer C., 2009, MNRAS, 399, L156
Rosswog S., Kasen D., Guillochon J., Ramirez-Ruiz E., 2009, ApJ, 705, L128
Rothman L. S. et al., 2009, J. Quant. Spectrosc. Radiat. Transfer, 110, 533
Shen K. J., Guillochon J., Foley R. J., 2013, ApJ, 770, L35
Simon J. D. et al., 2007, ApJ, 671, L25
Simon J. D. et al., 2009, ApJ, 702, 1157
Sparks W. M., Stecher T. P., 1974, ApJ, 188, 149
Spitzer L., 1978, Physical Processes in the Interstellar Medium. Wiley, New York
Sternberg A. et al., 2011, Science, 333, 856 (S11)
Stritzinger M. D. et al., 2011, AJ, 142, 156
Sullivan M. et al., 2010, MNRAS, 406, 782
Thompson T. A., 2011, ApJ, 741, 82
Vogt S. S. et al., 1994, in Crawford D. L., Craine E. R., eds, Proc. SPIE Conf. Ser. Vol. 2198, Instrumentation in Astronomy VIII. SPIE, Bellingham, p. 362
Wang X., Wang L., Filippenko A. V., Zhang T., Zhao X., 2013, Science, 340, 170
Webbink R. F., 1984, ApJ, 277, 355
Whelan J., Iben I., Jr, 1973, ApJ, 186, 1007
Yamanaka M., Ui T., Arai A., 2011, Cent. Bur. Electron. Telegrams, 2943, 3
Yusa T. et al., 2012, Cent. Bur. Electron. Telegrams, 3349, 1
Zhang T.-M., Lin M.-Y., Wang X.-F., 2012, Cent. Bur. Electron. Telegrams, 3146, 3

APPENDIX A: DESCRIPTION OF THE OBSERVATIONS

In this appendix, we provide information regarding the discovery and spectroscopic observations of each SN in the presented sample.

SN 2007on was discovered on 2007-11-05.25 UT (all dates in this paper are given in UT) 12″west and 68″north of the centre of the elliptical galaxy NGC 1404 (Pollas & Klotz 2007) and reported to be a young SN Ia on 2007-11-06 (Gal-Yam et al. 2007). Based on the Carnegie Supernova Project photometric data[2] SN 2007on maximum light in *B* band occurred around 2007-11-16. HIRES spectra of SN 2007on were obtained on 2007-11-20.3 and 2008-01-16.2. The first observation was performed 4 d after *B* band maximum light.

SN 2007sa was discovered on 2007-11-21.56 1.″8 west and 7.″7 north of the nucleus of NGC 3499 (Mostardi & Li 2007) and reported to be an SN Ia one month after maximum light on 2007-12-12.14 (Agnoletto et al. 2007). HIRES observations of SN 2007sa were performed on 2008-01-17.4 and 2008-01-23.59. Both spectroscopic epochs were obtained quite late (the first one 66 d after maximum light) and fairly close together, reducing the sensitivity to variable absorption.

SN 2007sr was discovered on 2007-12-18.53 on the southern arm of the antennas galaxies emanating from NGC 4038 (Drake et al. 2007), at 4 d after maximum light (Pojmanski et al. 2008). SN 2007sr was classified as an SN Ia on 2007-12-19 (Naito et al. 2007). SN 2007sr was observed using MIKE on 2007-12-20, 2007-12-21, and 2007-12-22, using EAE on 2007-12-24, and using HIRES on 2008-01-17. The first epoch was obtained around 6 d after maximum light.

SN 2008C was discovered on 2008-01-03.27 2.″95 west of the centre of UGC 3611 (Puckett et al. 2008) and confirmed as an SN Ia near maximum light on 2008-01-04.8 (Ayani & Yamaoka 2008). SN 2008C was observed using HIRES on 2008-01-17.64 and 2008-01-23.55. SN 2008C was spectrally typed as a normal Type Ia (Stritzinger et al. 2011). The first epoch observation was performed 16 d after maximum light (Foley et al. 2012).

SN 2008dt was discovered on 2008-06-30.33 1.″0 east and 5.″5 south of the nucleus of NGC 6261 (Madison, Li & Filippenko 2008) and confirmed as an SN Ia around one week before maximum light on 2008-07-01.21 (Blondin & Berlind 2008). SN 2008dt was observed using HIRES on 2008-07-06.48, 2008-07-12.48 and 2008-07-18.46. The first epoch observation was performed 6 d after maximum light (Foley et al. 2012).

SN2009ds was discovered on 2009-04-28.56 12″west and 3″north of the centre of NGC 3905 (Nakano et al. 2009) and confirmed as a normal SN Ia around one week before maximum light on 2009-04-29.6 (Anderson et al. 2009; Challis & Calkins 2009). MIKE observations of SN 2009ds were performed on 2009-05-15.96 and 2009-06-01.97. The first epoch observation was performed around 7 d after maximum light.

SN 2010A was discovered on 2010-01-04.14 2.″4 east and 6.″9 north of the centre of UGC 2019 (Cox et al. 2010), and classified as a normal Type Ia at 9 d before maximum brightness on 2010-01-07 (Foley & Esquerdo 2010). SN 2010A was observed with MIKE on 2010-01-08, 2010-01-09, and 2010-01-30. The first epoch spectrum was obtained about 8 d before maximum light.

SN 2011iy was discovered on 2011-12-09.86 16.″6 east and 6.″1 south of the centre of NGC 4984 (Itagaki et al. 2011), and classified as a Type Ia at 12 d after maximum light on 2011-12-14.81 (Yamanaka, Ui & Arai 2011). SN 2011iy was observed with MIKE on 2012-02-04.26 and 2012-06-06.12. The first epoch spectrum was obtained about 64 d after maximum light.

SN 2012cu was discovered on 2012-06-11.1 3.″1 east and 27.″1 south of the nucleus of NGC 4772 (Itagaki et al. 2012), and was classified as an SN Ia 7 d before maximum light (Marion et al. 2012; Zhang, Lin & Wang 2012). MIKE observations were performed on 2012-06-30.01 and 2012-07-16.03. UVES observations were performed on 2012-07-28.99 and 2012-08-10.98. The first epoch observation was performed around 8 d after maximum light.

SN 2012fr was discovered on 2012-10-27.05 3″west and 52″north of the nucleus of NGC 1365 (Klotz et al. 2012), and classified as a Type Ia on 2012-10-28.53 (Childress et al. 2012). Observations with UVES were performed on 2012-11-07.16, 2012-11-19.08, 2012-12-02.13 and 2012-12-21.05, and with MIKE on 2013-02-16.01.

[2] http://csp.obs.carnegiescience.edu/data/lowzSNe/SN2007on/

The first epoch spectrum was obtained around about 5 d before maximum light.

SN 2012hr was discovered on 2012-12-16.533 2.″3 west and 93.″6 north of the centre of ESO 121-26 (Drescher et al. 2012). SN 2012hr was classified as an SN Ia approximately 1 week before maximum light on 2012-12-20.2 (Morrell et al. 2012). MIKE observations were performed on 2013-01-02 and 2013-02-01. The first epoch spectrum was obtained about 7 d after maximum light.

SN 2012ht was discovered on 2012-12-18.77 19″ west and 16″ north of the centre of NGC 3447 and classified as an SN Ia 7 d before maximum light on 2012-12-20.4 (Yusa et al. 2012). Based on *Swift* light curves maximum light occurred around 2013-01-04.[3] Observations with MIKE were performed on 2013-01-02.29 and 2013-01-11.33, and with UVES on 2013-01-09.34, 2013-01-16.34 and 2013-01-28.28. The first epoch observation was performed around 2 d before maximum light.

2013aa was discovered 2013-02-13.62 74″ west and 180″ south of the centre of NGC 5643 (Parker et al. 2013). SN 2013aa was classified as a Type Ia a few days before maximum light on 2013-02-15.38 (Parrent et al. 2013). SN2013aa was observed with MIKE on 2013-02-16.38 and with UVES on 2013-02-24.31, 2013-03-01.31, 2013-03-11.39 and 2013-04-14.3. The first epoch spectrum was obtained about 1 d before maximum light.

2013aj was discovered on 2013-03-03.14 5.″7 east and 8″ north of the centre of NGC 5339 and was classified on the same night as an SN Ia 7 d before maximum light (Brimacombe et al. 2013). Observations with UVES were performed on 2013-03-13.29 and 2013-04-14.24. The first epoch observation was performed around 3 d after maximum light.

[3] http://people.physics.tamu.edu/pbrown/SwiftSN/SN2012ht_lightcurve.jpg

This paper has been typeset from a TEX/LATEX file prepared by the author.